Robust Separation of Visceral and Subcutaneous Adipose Tissues in Micro-CT of Mice

Bibo Shi[1] Shuisheng Xie[1] Darlene Berryman[2] Ed List[2] Jundong Liu[1]
[1] School of Electrical Engineering and Computer Science
[2] Edison Biotech Institute
Ohio University, Athens, OH 45701, USA

***Abstract*— One of the common practices in obesity and diabetes studies is to measure the volumes and weights of various adipose tissues, among which, visceral adipose tissue (VAT) and subcutaneous adipose tissue (SAT) play critical yet different physiological roles in mouse aging.**

In this paper, a robust two-stage VAT/SAT separation framework for micro-CT mouse data is proposed. The first stage is to distinguish adipose from other tissue types, including background, soft tissue and bone, through a robust mixture of Gaussian model. Spatial recognition relevant to anatomical locations is carried out in the second step to determine whether the adipose is visceral or subcutaneous. We tackle this problem through a novel approach that relies on evolving the abdominal muscular wall to keep VAT/SAT separated. The VAT region of interest (ROI) is also automatically set up through an atlas based skeleton matching procedure.

The results of our method are compared with VAT/SAT delineations by human experts, and a high classification accuracy is demonstrated on eight micro-CT mouse volume sets.

I. Introduction

Excess abdominal adipose tissue is associated with increased risk of cardiovascular and metabolic aberrations of obesity, diabetes and coronary artery diseases. Accurate measurement of adipose tissue distribution based on small animal imaging devices, including magnetic resonance imaging (MRI) and computerized tomography (CT), would offer a useful insight when studying these diseases and evaluating the efficacy of treatment compounds using small animal subjects.

Among various adipose types, visceral adipose tissue (VAT) and subcutaneous adipose tissue (SAT) play particularly critical yet different physiological roles in various disease procedures. While both VAT and SAT have been associated with many metabolic risk factors including fasting plasma insulin, triglycerides, low-density lipoprotein, or cholesterol levels, VAT is more closely correlated with coronary artery diseases or diabetes, and therefore more predictive of obesity-induced pathologies than whole body adipose tissue and SAT.

The past ten years have seen the development of a number of automatic VAT/SAT separation algorithms [1], [2], [3], [4], [5], [6], which usually involve two major analysis tasks. The first step is adipose extraction, i.e. distinguishing fat from other tissues. Various voxel classification based on single or multi-channel intensity values [7] have been utilized to tackle this problem. Commonly modeled with certain parametric voxel statistics, these methods estimate the distribution profile of each class based on image pixel intensities, and classification is carried out according to the probability value of each individual pixel. With respect to the form of the probability density function, finite Gaussian mixture models [8], [9], [10] has been widely assumed in many segmentation models.

The second step is to further classify the fat into subcutaneous or visceral based on relative anatomical locations with respect to the abdominal muscular wall. Region-growing algorithms [11] start from manually or automatically planted seed points in different fat regions, and iteratively propagate memberships to nearby voxels according to their similarity in intensities and proximity in locations. The expansion will stop when the similarity falls below certain threshold in nearby regions. Another group of solutions locate SAT and VAT through the tracking of the abdominal muscular wall. The wall is beneath the subcutaneous fat, which is visible in any given trans-axial slice; thus, evolving the wall along the slice stack will result in enclosed VAT area. Edge-based [5], [12], [13] and region-based [6] active contour models fit in well to achieve this goal. However, the contour-based wall-tracking approaches for VAT/SAT separation tend to suffer from weak boundary as well as edge leakage problem. In order to keep the contour faithfully aligned with the actual muscle wall, extra care needs to be taken to avoid the curve bending into VAT areas. In addition, with the exception of [6], most published works in the literature rely on user intervention to manually choose the starting and ending slices that define the VAT region of interest (ROI).

A. Proposed method

In this paper, we present a robust VAT/SAT separation framework to address the aforementioned issues. In the fat/non-fat separation step, we adopt a robust finite Gaussian mixture classification method to accurately capture the fat tissues. To propagate the abdominal wall for VAT/SAT delineating, a deformable registration is applied along slice stack to ensure a robust and smooth region tracking. Through an atlas-based skeleton matching procedure, a fully automatic VAT ROI setup has been implemented by locating the T10 and L5 vertebrae.

II. Methods

In this section, we illustrate our VAT/SAT separation framework in the order: 1) robust fat/non-fat separation based a mixture of Gaussian model; 2) VAT/SAT separation through wall evolution; 3) VAT ROI set up based on bone signature and 4) segmentation result validation with semi-automatic results as the gold standard.

A. Fat/non-Fat separation based L_2E

To separate fat and non-fat areas in micro-CT data, we adopt a robust finite Gaussian mixture (FGM) segmentation method, where the fitting criterion is defined as the squared difference between the true density and the assumed Gaussian mixture.

Suppose $y(x)$ is an unknown density function. The parametric approximation of $y(x)$ is $\hat{y}(x|\theta)$. The L_2E minimization estimator for θ is given as:

$$\begin{aligned}\hat{\theta}_{L_2E} &= \arg\min_{\theta} \int [\hat{y}(x|\theta) - y(x)]^2 dx \qquad (1)\\ &= \arg\min_{\theta} \int [\hat{y}^2(x|\theta) - 2\hat{y}(x|\theta)y(x) + y^2(x)]dx\end{aligned}$$

Let $\phi(x|\boldsymbol{\mu}, \boldsymbol{\sigma})$ denotes the univariate normal density, the parametric distribution assumed by FGMs is as follows:

$$y(x|\boldsymbol{\theta}) = \sum_{k=1}^{K} w_k \phi(x|\mu_k, \sigma_k) \qquad (2)$$

where $\boldsymbol{\theta} = \{\boldsymbol{w}, \boldsymbol{\mu}, \boldsymbol{\sigma}\}$ is a combined vector representing the portions, means, and standard deviations of the Gaussian components.

Expectation-Maximization (EM) algorithm, the estimator of the Maximum Likelihood (ML) measure, has been widely used in many FGM-based segmentation algorithms. However, ML, together with EM, is inherently not robust and potentially influenced by input outliers. Our robust model is formulated as a special case of Eqn. (1), where $\hat{y}(x|\theta)$ is a mixture of Gaussians. Comparing with the popular ML (EM) measure, our solution has the advantage of being able to capture target structures accurately, without being affected by the outlier components. For more details, we refer the readers to [14].

B. VAT/SAT separation through deformable registration along slice stack

After the overall fat tissues are obtained, further separating the areas into SAT and VAT can be achieved by propagating the abdominal wall along axial slices. Currently, most solutions model the wall as a sequence of closed 2D contours, which can be tracked through a curve evolution procedure. However, due to the vast elasticity allowed for the curves, the evolution procedure tends to deviate from the course and get trapped into interior areas of VAT, especially when weak edges are encountered.

Our wall tracking solution is to replace slice-wise curve evolution with slice-wise registration, and the justification is twofold. On one hand, deformable registration keeps track of the corresponding structures in neighboring slices, therefore helps achieve the goal of morphing and extracting the abdominal wall. On the other hand, with an imposed smoothness constraint to the deformation field, the evolutions of the wall are confined within certain limits, which puts a safeguard to prevent the placements of the evolving wall from vastly deviating off the target.

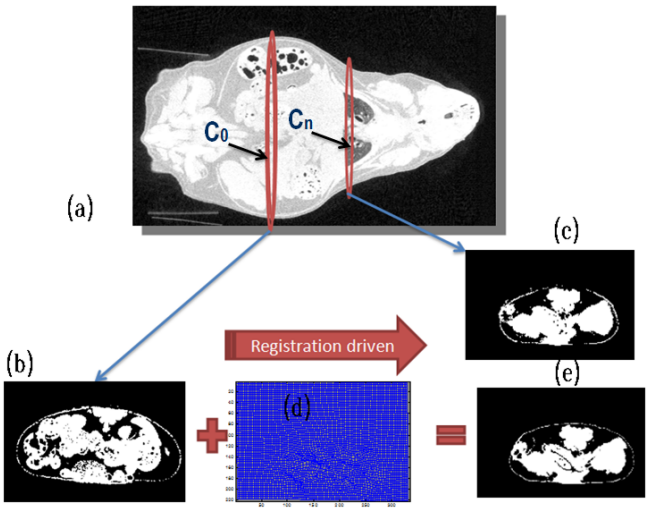

Fig. 1. Illustration of the abdominal wall evolution procedure. Please refer to text for details.

Fig. 1 illustrates the procedure. A central slice extracted around the mid point of the body, together with its lean tissue, was chosen as the starting point. The lean tissue is a "by-product" of the fat/non-fat separation procedure. The abdominal wall contour, a sequence of points, can be easily obtained through a morphological operation performed on the boundary of the lean tissue. Two registration progressions are subsequently conducted towards opposite directions along the axial slice stack. In our study, the Demons' algorithm is adapted as the underlying deformable registration solution.

Fig. 1(a) is an illustration of the overall wall evolution procedure. Fig. 1(b) is the lean portion within the central slice C_0 and C_n is another slice, which could be the immediate neighbor of C_0. Fig. 1(e) is the transformed C_0 after applying the estimated deformation Fig. 1(d) between (b) and (c). Evolution of the abdominal wall is achieved by repeatedly conducting the registration & transformation steps for neighboring slices.

C. VAT region of interest (ROI) setup based on skeleton atlas

To automatically decide the region of interest (ROI) of VAT is a challenging problem for mouse subjects. A number of solutions have been reported to tackle this issue through the utilization of bone index [2] and adipose/lean amount [6].

We adopt a commonly accepted bone signature criterion [2] to set up the VAT ROI — it should cover the entire abdominal cavity (slices spanning between the proximal end

of the T10 vertebra and the distal end of the L5 vertebra). To automate the ROI selection procedure, we employ an atlas based approach, where the atlas was an arbitrarily chosen mouse from our experiment data set. The ROI of the atlas was manually set by specifying the starting and ending slices of the T10 and L5 vertebrae. Other mice's ROIs are decided through a skeleton matching w.r.t. to the atlas. The procedure starts with skeleton centerline extraction based on a fast marching method [15]. Then, the skeletons of each input mouse and the atlas are matched through a robust point registration algorithm [16]. With the matched spines, the T10 and L5 vertebrae of each mouse can be easily localized. Fig. 2 shows the skeleton registration and ROI identification procedure (the bottom mouse is the atlas).

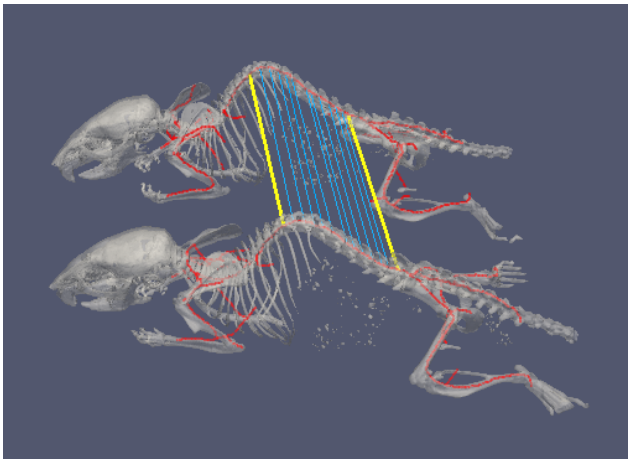

Fig. 2. VAT ROI localization: the volume between the two yellow lines is the ROI (T10-L5).

D. Validation based on semi-manual ground truth

To evaluate the accuracy and robustness of our VAT/SAT separation framework, semi-manual analysis from trained operators was considered as the ground truth segmentation and used as a reference.

The semi-manual functionality is implemented within a three-view display software package, where the user can specify VAT boundary points by clicking on axial slices. The boundary points are expected to be placed around the centers of the abdominal contour, and a resampling & interpolation routine will be applied to densify the control points and generate a smooth yet faithful curve to separate the VAT & SAT areas.

With the semi-manual results available as the ground truth, we can assess the accuracy and consistency of our segmentation results through a comparison between the automatic and semi-manual segmentations. The performance metrics used in our study include: *Correlation Coefficient, Dice Coefficient, Sensitivity and Specificity*. Dice coefficient measures the similarity of two sets and ranges from 0 for sets that are disjoint to 1 for sets are identical.

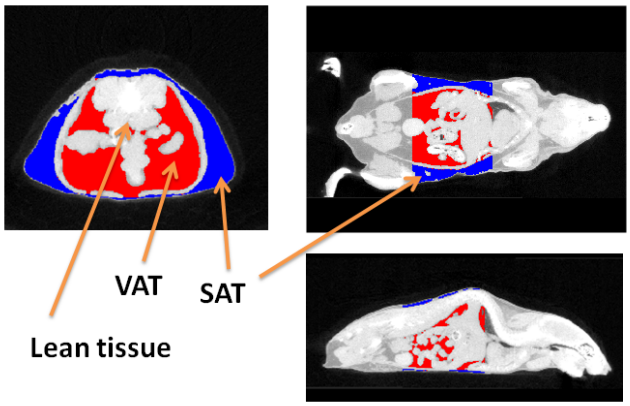

Fig. 3. Three-view display of a VAT/SAT separation result generated from our framework. Blue and red areas correspond to the extracted SAT and VAT, respectively.

III. Experimental Results

The experiment we conducted was based on 8 sets of micro-CT mouse images provided by Edison Institute at Ohio University. The data sets were obtained using the GE eXplore Locus Small Animal MicroCT Scanner (GE Healthcare, London, Ontario, Canada) with a 95-micron voxel protocol with the following scan parameters: 80 kV, 450 m A, and 2000-milliseconds exposure time. The mice, ranging from 9 to 12 months old, are C57BL/6J background.

Fig. 3 shows one of the subjects and the separation result. Blue and red areas correspond to the extract SAT and VAT, respectively. It should be noted that with the presence of a very thin and even disappearing abdominal wall lying between SAT and VAT, primitive segmentation methods, such as intensity thresholding, or region-growing algorithms, would not be sufficient to achieve the goal.

A. Statistical Analysis for VAT/SAT separation

Due to the huge number of slices in each mouse data set (on average, the VAT ROI spans 200 slices), semi-manual segmentation was performed on sampled slices instead of the entire volume. For each mouse data set, we sampled ten slices that are roughly even-spaced within the VAT ROI area. Evaluation of the VAT/SAT segmentation accuracy and consistency was carried out based on the sampled slices. Automatic segmentation results were compared with the semi-manual ground truth, and statistical analysis were conducted accordingly.

The *correlation coefficients* estimated from the eight data sets is shown in Fig. 4. For SAT, the coefficient R^2 is 0.994, and for VAT, 0.996, with confidence level of 95% . Both are very close to 1, which indicates our automatic results are highly aligned with the semi-manual ground truth.

Other performance metrics results are shown in Table 1, inculding Dice coefficient (DC.), Sensitivity (Sensi.), and Specificity (Speci.). The average Dice coefficient (similarity index) for the eight mice data sets for SAT is 0.9690; for VAT, is 0.9753 respectively, which are higher than the

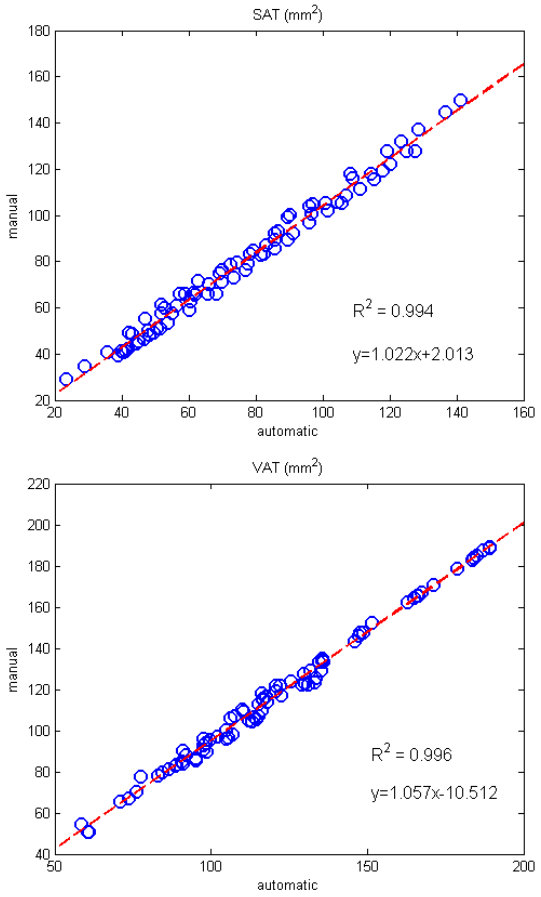

Fig. 4. Correlation of automatic and semi-manual results in SAT and VAT.

reported numbers in two published work [4], [5]. Although no direct comparison with other works can be made at this point due to the different testing data used, the high similarity indexes obtained are good indications of the accuracy and robustness of our solution.

Set	DC. [SAT]	DC.[VAT]	Sensi. [SAT]	Speci. [SAT]
1	0.9439	0.9525	0.9237	0.9974
2	0.9549	0.9537	0.9224	0.9891
3	0.9514	0.9655	0.9188	0.9905
4	0.9579	0.9613	0.9131	0.9947
5	0.9862	0.9874	0.9814	0.9919
6	0.9898	0.9942	0.9808	0.9904
7	0.9850	0.9922	0.9822	0.9937
8	0.9830	0.9956	0.9806	0.9963
Ave.	0.9690	0.9753	0.9504	0.9930
STD.	0.0187	0.0188	0.0332	0.0030

TABLE I

PERFORMANCE METRICS BETWEEN AUTOMATIC SEGMENTATION RESULTS AND SEMI-MANUAL GROUND TRUTH. (NOTE: SINCE THE SAT AND VAT ARE MUTUALLY EXCLUSIVE AND EXHAUSITIVE WITHIN THE TOTAL ANDIPOSE TISSUE, THE SENSITIVITY AND SPECIFICITY FOR VAT ARE IDENTICAL TO THE SPECIFICITY AND SENSITIVITY FOR SAT.)

IV. CONCLUSIONS

We have described a fully automatic framework for VAT/SAT adipose tissue separation that requires virtually no user intervention. Two tasks are involved, first fat/non-fat and then VAT/SAT separation, and the evolution procedure can terminate at the end of VAT area due to an automated ROI setup mechanism. The novelty of our solution for the second step lies in the fact that a regularity-guaranteed registration algorithm can very well impose global control over the curve evolution procedure. Extending the current model to handle other tissue/organ segmentation, as well as various pathology dection are among our planned work.

REFERENCES

[1] S. Lublinsky, Y.K. Luu, C.T. Rubin, and S. Judex, "Automated separation of visceral and subcutaneous adiposity in in vivo microcomputed tomographies of mice," *Journal of Digital Imaging*, vol. 22, no. 3, pp. 222–231, 2009.

[2] S. Judex, YK Luu, E. Ozcivici, B. Adler, S. Lublinsky, and CT Rubin, "Quantification of adiposity in small rodents using micro-ct," *Methods*, vol. 50, no. 1, pp. 14–19, 2010.

[3] P. Ranefall, A.W. Bidar, and P.D. Hockings, "Automatic segmentation of intra-abdominal and subcutaneous adipose tissue in 3d whole mouse mri," *Journal of Magnetic Resonance Imaging*, vol. 30, no. 3, pp. 554–560, 2009.

[4] Y. Tang, P. Sharma, M.D. Nelson, R. Simerly, and R.A. Moats, "Automatic abdominal fat assessment in obese mice using a segmental shape model," *Journal of Magnetic Resonance Imaging*, 2011.

[5] B. Zhao, J. Colville, J. Kalaigian, S. Curran, L. Jiang, P. Kijewski, and L.H. Schwartz, "Automated quantification of body fat distribution on volumetric computed tomography," *Journal of computer assisted tomography*, vol. 30, no. 5, pp. 777, 2006.

[6] A. Marchadier, C. Vidal, J.P. Tafani, S. Ordureau, R. Lédée, C. Léger, et al., "Quantitative ct imaging for adipose tissue analysis in mouse model of obesity," *SPIE MI*.

[7] T. Yang, L. Susan, N. Marvin, R. Simerly, and M. Rex, "Adipose segmentation in small animals at 7t: a preliminary study," *BMC Genomics*, vol. 11.

[8] R. Guillemaud and M. Brady, "Estimating the bias field of mr images," *Medical Imaging, IEEE Transactions on*, vol. 16, no. 3, pp. 238–251, 1997.

[9] K. Held, E.R. Kops, B.J. Krause, W.M. Wells III, R. Kikinis, and H.W. Muller-Gartner, "Markov random field segmentation of brain mr images," *Medical Imaging, IEEE Transactions on*, vol. 16, no. 6, pp. 878–886, 1997.

[10] A. Mechelli, C.J. Price, K.J. Friston, and J. Ashburner, "Voxel-based morphometry of the human brain: methods and applications," *Current Medical Imaging Reviews*, vol. 1, no. 2, pp. 105–113, 2005.

[11] A. Tsai, A. Yezzi Jr, W. Wells, C. Tempany, D. Tucker, A. Fan, W.E. Grimson, and A. Willsky, "A shape-based approach to the segmentation of medical imagery using level sets," *Medical Imaging, IEEE Transactions on*, vol. 22, no. 2, pp. 137–154, 2003.

[12] S. Ohshima, S. Yamamoto, T. Yamaji, M. Suzuki, M. Mutoh, M. Iwasaki, S. Sasazuki, K. Kotera, S. Tsugane, Y. Muramatsu, et al., "Development of an automated 3d segmentation program for volume quantification of body fat distribution using ct," *Japanese Journal of Radiological Technology*, vol. 64, no. 9, pp. 1177–1181, 2008.

[13] V. Positano, T. Christiansen, M.F. Santarelli, S. Ringgaard, L. Landini, and A. Gastaldelli, "Accurate segmentation of subcutaneous and intermuscular adipose tissue from mr images of the thigh," *Journal of Magnetic Resonance Imaging*, vol. 29, no. 3, pp. 677–684, 2009.

[14] Shuisheng Xie, Jundong Liu, Darlene E. Berryman, Edward O. List, Charles Smith, and Hima Chebrolu, "A robust image segmentation model based on integrated square estimation," in *ISVC (2)*, 2007, pp. 643–651.

[15] R. Van Uitert and I. Bitter, "Subvoxel precise skeletons of volumetric data based on fast marching methods," *Medical physics*, vol. 34, pp. 627, 2007.

[16] A. Myronenko and X. Song, "Point set registration: Coherent point drift," *Pattern Analysis and Machine Intelligence, IEEE Transactions on*, vol. 32, no. 12, pp. 2262–2275, 2010.